Biomed Microdevices (2011) 13:485–491
DOI 10.1007/s10544-011-9516-8

Micro-fabricated perforated polymer devices for long-term drug delivery

Zhuo-Jie Wu · Zhiquan Luo · Ashish Rastogia · Salomon Stavchansky · Phillip D. Bowman · Paul S. Ho

Published online: 24 February 2011

Abstract Fabrication techniques have been developed to produce a perforated polymer microtube as a drug delivery device. The technique consists of first forming a silicon platform with trenches and alignment marks to hold the tubes for subsequent processing. Photolithography and reactive ion etching with an inductively coupled plasma source were used to fabricate micro holes on the surface of polyimide tubes. Several materials have been used to form the etching mask, including titanium film deposited by e-beam evaporation and SiO_2 and SiN_x films deposited by high-density plasma chemical vapor deposition (HDPCVD). Three equidistant holes of 20 μm in diameter were fabricated on polyimide tubes (I.D. = 125 μm). The perforated tubes were loaded with ethinyl estradiol and tested for drug release in phosphate buffered saline (pH=7.1) at 37°C. Zero order release was observed over a period of 30 days with a potential to be extended to 4 years.

Keywords Drug delivery device · Microfabrication · Polymer tube · Polyimide

Zhuo-Jie Wu and Zhiquan Luo contributed equally to this work.

Z.-J. Wu · Z. Luo · P. S. Ho (✉)
Microelectronics Research Center,
The University of Texas at Austin,
Austin, TX 78758, USA
e-mail: paulho@mail.utexas.edu

A. Rastogia · S. Stavchansky
Division of Pharmaceutics, College of Pharmacy,
The University of Texas at Austin,
Austin, TX 78712, USA

A. Rastogia · P. D. Bowman
U.S. Army Institute of Surgical Research,
San Antonio, TX 78234, USA

1 Introduction

Drug efficacy and safety can be improved by delivering the drug locally to a targeted site at a controlled rate. Controlled release of drugs helps to keep the active agent concentration in the local environment within the therapeutic range to avoid toxicity and also to maximize the therapeutic effect (Baker 1987; Hillery et al. 2001; Robinson and Lee 1987). Compared to conventional forms of delivery, such as injections or oral formulations, implantable drug delivery systems can deliver drugs locally so that biological and/or metabolic barriers to the drug can be avoided and drugs can be released with a higher efficiency. In addition, the amount of dose needed and the side effects are also reduced.

We have recently described the concept of drug delivery and release from a microperforated device (Rastogi et al. 2010) that is capable of long term zero order release. The device consists of a reservoir for the storage of the drug of interest and a small hole on the surface makes possible dissolution of the drug that is released at a rate dependent on its solubility characteristics. The device may be used for the management of chronic conditions wherein long term drug therapy is needed. The two sets of microperforated tubes that were used in a previous study were manufactured using laser drilling or drill bits. In this study, we demonstrate the manufacturing of the microperforated microdevice using a photolithographic process.

During the past decades, the application of silicon microfabrication technology in drug delivery devices has gained extensive interests (Maloney et al. 2005; Martin et al. 2005; Desai et al. 1999; Santini et al. 1999, 2000). The feasibility of integration of such devices with microelectronics, biosensors and wireless control have demonstrated excellent potentials to bring the drug delivery to a whole new level of applications (Santini et al. 2000; Tang et al. 2008).

Report Documentation Page

Form Approved
OMB No. 0704-0188

1. REPORT DATE	2. REPORT TYPE	3. DATES COVERED
01 JUN 2011	**N/A**	**-**

4. TITLE AND SUBTITLE	5a. CONTRACT NUMBER
Micro-fabricated perforated polymer devices for long-term drug delivery	5b. GRANT NUMBER
	5c. PROGRAM ELEMENT NUMBER
6. AUTHOR(S)	5d. PROJECT NUMBER
Wu Z. J., Luo Z., Rastogi A., Stavchansky S., Bowman P. D., Ho P. S.,	5e. TASK NUMBER
	5f. WORK UNIT NUMBER
7. PERFORMING ORGANIZATION NAME(S) AND ADDRESS(ES)	8. PERFORMING ORGANIZATION REPORT NUMBER
United States Army Institute of Surgical Research, JBSA Fort Sam Houston, TX	
9. SPONSORING/MONITORING AGENCY NAME(S) AND ADDRESS(ES)	10. SPONSOR/MONITOR'S ACRONYM(S)
	11. SPONSOR/MONITOR'S REPORT NUMBER(S)

12. DISTRIBUTION/AVAILABILITY STATEMENT
Approved for public release, distribution unlimited

13. SUPPLEMENTARY NOTES

14. ABSTRACT

15. SUBJECT TERMS

16. SECURITY CLASSIFICATION OF:			17. LIMITATION OF ABSTRACT	18. NUMBER OF PAGES	19a. NAME OF RESPONSIBLE PERSON
a. REPORT	b. ABSTRACT	c. THIS PAGE			
unclassified	**unclassified**	**unclassified**	**UU**	**8**	

Standard Form 298 (Rev. 8-98)
Prescribed by ANSI Std Z39-18

However, several disadvantages limit the use of silicon in practice. Unlike polymeric material, silicon is rigid and brittle which may result in tissue damage and possible device breakdown after implantation and also bulk silicon has biocompatibility issues (Voskerician et al. 2003).

In this paper, we have developed a method to apply the micro-fabrication technology to fabricate drug delivery devices using polymer micro-tubes, thus taking advantage of both polymer material and micro-fabrication technology while avoiding the shortcomings of material properties of silicon and conventional manufacturing methods. We have used a biocompatible polymer (polyimide) to serve as a reservoir and photolithographically produced microholes for the release of the drug. The device design is schematically shown in Fig. 1, wherein, the microholes for drug release fabricated on one surface of the polymer tube are illustrated. The wall of micro-tube is impermeable to the drug. The two ends of microtubes are sealed after drug loading. Long-term zero order drug release was achieved with such devices. The release rate can be readily tuned by changing the number or the area of the microholes.

2 Experimental section

2.1 Device fabrication

The micro-tubes used in this study were polyimide tubes from Microlumen Inc. (Tampa, FL, USA). Polyimide is a biocompatible polymer formed from an imide family of monomers (Rousche et al. 2001; Niwa et al. 2001). Due to its high mechanical toughness, thermal stability and chemical resistance, polyimide is widely used in micro-electronics industry (Bessonov et al. 1987; Feger et al. 1996). The outside diameter of tubes used was 165 μm with a wall thickness of 20±6 μm. There were several material and processing issues which had to be solved in order to fabricate microholes on the polyimide tubes using the microfabrication technology. Small tubes are hard to handle and cylindrical microtubes offered additional challenge as the current microfabrication is developed primarily for planar substrates. In addition, current etching techniques in microelectronics deal with etching processes to depth usually below 1 μm while here we need to etch through the tube wall with thickness around 20 μm.

Fig. 1 The drug delivery device in form of a cylindrical tube with microholes on one side of the tube surface

2.1.1 A silicon platform

To facilitate handling of the polyimide tubes, a platform was developed that consists of a silicon wafer with trenches and alignment marks on its surface. The trenches were designed to be slightly bigger than the tubes so that tubes can fit into them. Alignment marks were designed to position the micro-hole patterns to the desired position on the polyimide tubes. A combination of photolithography and silicon wet anisotropic etching was applied to fabricate the silicon platform. A schematic process flow is shown in Fig. 1(a). It starts with a thermal growth of a SiO_2 layer on a (110) Si wafer followed by an e-beam deposition of a Cr layer on top. After spin-coating a photo-resist (AZ 5209E) layer, photolithography was used to define the trench patterns and the alignment marks. All photolithography in this study was done using an EVG620 Mask Aligner in a hard contact mode with an i-line (365 nm) source. The direction of trenches was aligned to the <112> direction, so that vertical trenches can be formed using a wet anisotropic etching (Li et al. 2008). We found that the vertical trenches can hold the polyimide tubes more tightly than the V-grooves etched from (100) Si wafer. A Cl_2/O_2 plasma was then applied to etch the patterns through the Cr layer followed by a CHF_3/O_2 plasma to etch the patterns through the SiO_2 layer to expose the Si underneath. Then Si wet anisotropic etching was performed using a 25 wt.% tetramethylammonium hydroxide (TMAH) solution at 80°C. An etching depth close to the diameter of polyimide tube was required. TMAH was selected because it is compatible to CMOS process and the anisotropic etching can be accurately controlled. A schematic overview of the silicon platform is shown in Fig. 2(b). Figure 3(c) is a scanning electron microscopic (SEM) image of a vertical etched trench which shows very smooth sidewalls formed by the {111} crystalline planes.

Alternatively, trenches on silicon wafer can be made by deep reactive ion etching (DRIE). In this case, the trenches are vertical independent of the orientation of the wafer. The processes can be much simplified since the photo-resist itself can be used as etching mask for Si DRIE. This method, however, yields a structure with much rough sidewalls and trench bottoms.

2.1.2 Fabrication of micro-holes

The second stage of processing starts by inserting the polyimide tubes into the trenches on the Si platform. Adhesives are required to stick the tubes to the trenches, particularly during subsequent spin-coating of the photo-resist. Photo-resist is used to help fix the polyimide tubes in the trenches. The excessive photo-resist on the surface of silicon wafer and tubes is removed by thoroughly exposing

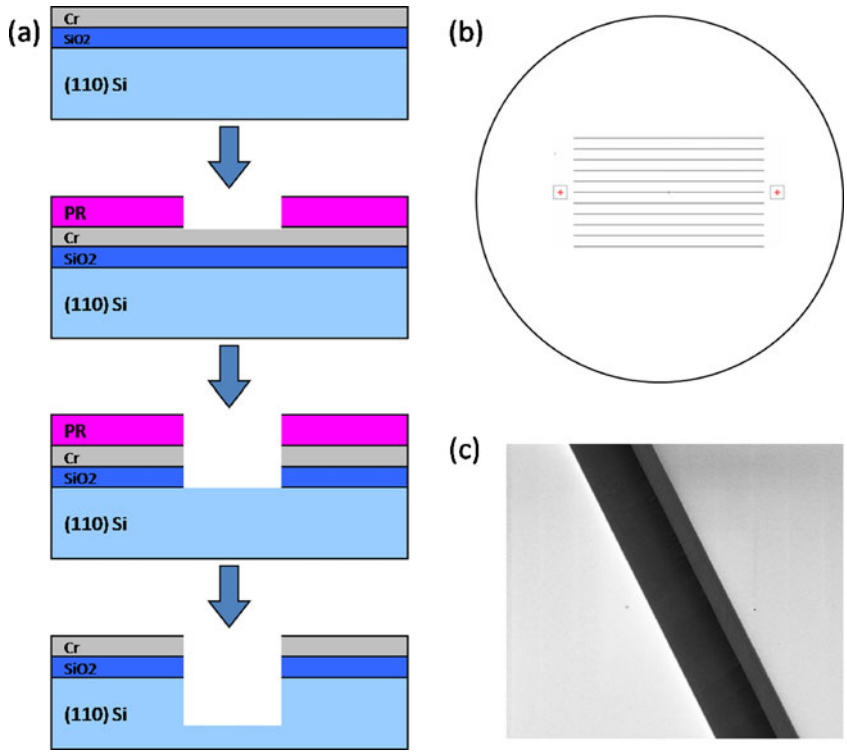

Fig. 2 (**a**) Process flow for fabrication of silicon platform; (**b**) schematic of a silicon platform following fabrication of a plurality of trench patterns and alignment marks; (**c**) a SEM image of a trench fabricated following process shown in (**a**)

the wafer under UV light to develop the exposed photo-resist, while the rest of the photo-resist underneath the tubes adhere the tubes in the trenches. The assembly of Si wafer and polyimide tubes is then handled as a conventional planar substrate for the subsequent processing steps.

Figure 3 shows the basic process flow for fabricating micro-holes after the polyimide tubes are inserted into the trenches. It starts with a deposition of mask material on the tube surface as shown in Fig. 3(a). Then photolithography is applied to define the micro-hole patterns on polyimide tubes with the help of the alignment marks on the Si platform, as shown in Fig. 3(b). An RIE step is applied to transfer the pattern through the mask film as shown in Fig. 3(c). Then an oxygen RIE is used to etch through the polyimide tube wall as shown in Fig. 3(d). Finally, the tubes are taken out and cleaned and the Si platform is reused for the next batch.

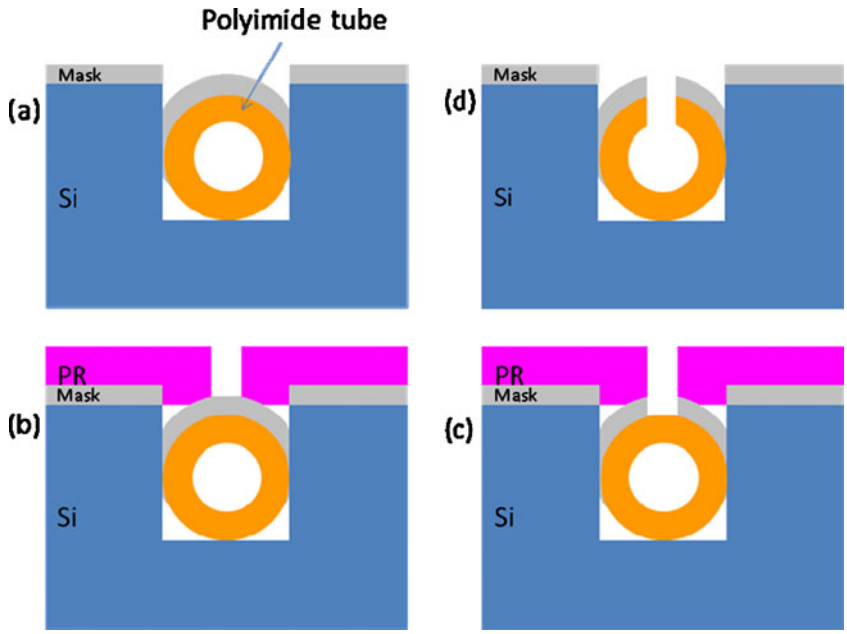

Fig. 3 Process flow for fabricating microholes on polyimide tubes in a Si platform

In this fabrication process, the tube wall thickness is close to 20 μm, hence the last step of oxygen RIE may take hours to etch through while conventional etching in microelectronics only takes minutes. This may cause problems such as local heating, sputtering and redeposition of the mask material and substrate charging. To solve these problems, an etcher with an inductively coupled plasma (ICP) RF power was used to tune the plasma density and ion energy. Although etching rate can be increased with RF power in a conventional etcher, the sputtering of energetic ions can cause severe sample damage if etched for a long time. While in an etcher with ICP source, the plasma density, which is normally much higher than conventional RIE, is separately controlled by ICP power. Higher etching rate can be achieved without severe sample damage by energetic ions. The tool used in this study was an Oxford Plasma Lab 80+ System. The etching was done with a RF power of 30 W and an ICP power of 300 W. The chunk was kept at 30°C by balancing the heating from a heating stage and the flow of liquid nitrogen.

2.1.3 Etching mask materials

Chromium, a widely used hard mask material in microfabrication, was used in this study. However, chromium is not biocompatible and hence is considered a contaminant that may lead to potential tissue toxicity problems. Titanium (Ti) is an excellent biocompatible material with a low sputtering yield as well indicating it is a suitable choice in the application here. Figure 4(a) shows an optical microscope image of a 20 μm hole etched on a polyimide tube using an e-beam evaporated Ti film as an etching mask. As we can see, the shape of hole is very circular. Holes with other shapes, e.g., square and slit, can be formed depending on the lithography pattern design. Figure 4(b) shows an image of a hole on tube after the Ti film is removed by Ti etchant. In our study, the top surface of polyimide tube was protected well by Ti mask. However the surface close to edges was partially etched by oxygen plasma, although it did not etch through. This may not be desirable for some applications. This problem may be caused by non-conformal mask deposition using e-beam evaporation. The problem can be solved using two mask deposition at oblique angles to cover each side of the tube.

Chemical vapor deposition (CVD) is a technique commonly used for conformal deposition (Ohring 2002) although the conventional CVD or PECVD (plasma enhanced CVD) process requires a temperature above 200°C. This can induced a thermal stress to strip the polyimide tube off the Si platform. Fortunately, this problem does not occur for the high density plasma (HDP) generated by the ICP source, where the deposition

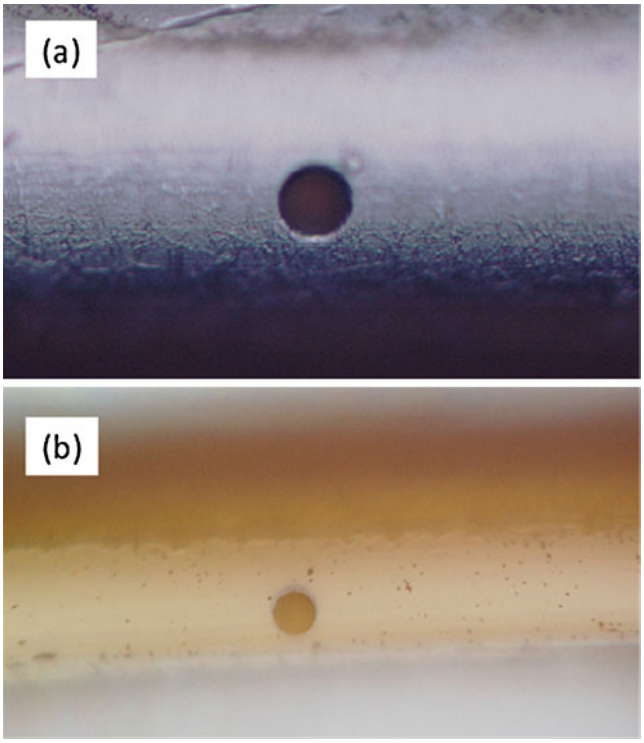

Fig. 4 (**a**) A 20 μm hole etched on a polyimide tube with Ti as etching mask; (**b**) an image showing the edge of tube surface isn't protected well

can be carried out at room temperature. Silicon dioxide (SiO_2) and silicon nitride (SiN_x) are two common materials that can be deposited by HDPCVD. Both of them are biocompatible (Voskerician et al. 2003) and can be used as etching masks for oxygen RIE. Figure 5 shows an image of a 20 μm hole etched on a polyimide tube with an etching mask of 150 nm SiO_2 deposited by HDPCVD at 30°C. The edges are well protected by the conformally deposited film. With this method, both mask film deposition and polyimide etching can be performed using the same tool to reduce capital equipment investment for manufacturing.

Occasionally, cracks were observed as shown in the inset of Fig. 5. Any crack on the polyimide tube surface corresponds to a crack formed first on the SiO_2 film. One common through-film crack is channel crack. It is well known that the energy release rate for channel crack of a film can be much enhanced if it is deposited on a compliant substrate compared to the one deposited on a stiff substrate (Hutchinson and Suo 1992; Tsui et al. 2005). The elastic modulus for polyimide is 7.5 GPa (Dolbow and Gosz 1996), while the modulus for SiO_2 film is 70 GPa (Tsui et al. 2005). Due to the elastic mismatch, the SiO_2 mask film is prone to crack.

One possible driving force for crack formation can be due to plasma-induced local heating during etching. Although the silicon substrate attached to the chunk was kept at 30°C throughout the etching, the local temperature

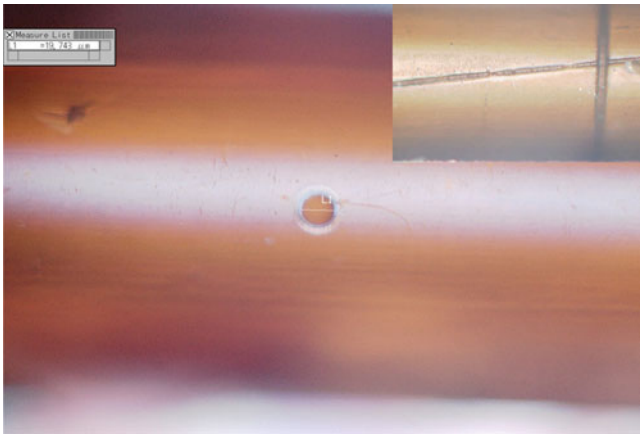

Fig. 5 A 20 μm hole etched on a polyimide tube with SiO_2 as etching mask. The inset shows cracks formed during etching

of the tube surface can be higher due to plasma induced local heating. This can give rise to a thermal stress due to thermal mismatching between the polyimide and oxide, which have CTE of 40 ppm/°C (MicroLumen http://www.microlumen.com/polyimide/material.html) and 0.5 ppm/°C (AZoM http://www.azom.com/Details.asp?ArticleID=1114) respectively. The tensile thermal stress can be sufficient to induce cracks first on the oxide mask and then transferred to the tube surface to form a crack as shown in Fig. 5.

For this reason, the silicon nitride film can be a better mask than silicon dioxide. We list the thermal and mechanical properties of both silicon dioxide and silicon nitride in Table 1. The CTE mismatch between silicon nitride and polyimide is smaller so that less stress will be induced. The thermal conductivity of silicon nitride is much higher than silicon dioxide, indicating that the heat generated during etching can be better dissipated by the nitride film to reduce the local heating and the crack driving force. In addition, the fracture toughness of silicon nitride is larger than that of silicon dioxide. The combination of these factors indicates that cracks are less likely to be generated on silicon nitride film than silicon dioxide film even if the same amount of stress is applied.

Figure 6 shows the result of the micro-hole formed using a silicon nitride mask. The mask was a 150 nm SiNx film deposited on the polyimide tube by HDPCVD at 30°C. Figure 6(a) and (b) are images of a 20 μm hole etched on a polyimide tube before and after the etching mask is removed. The SiN_x film masked both the top surface and edges of the polyimide tube very well and cracks were mostly suppressed. The tube surface after etching was as smooth as it was before processing. The diameter of the holes designed was 20 μm and the final diameter of holes after etching was checked by measurement using an optical microscope. The result illustrates a uniform lithography and etching process.

Table 1 Thermal and mechanical properties of silicon dioxide and silicon nitride (AZoM; Accuratus http://www.accuratus.com/silinit.html; Hatty et al. 2008)

	Silicon dioxide	Silicon nitride
CTE (ppm/°C)	0.5	3.2
Thermal Conductivity (W/m·°C)	1.4	30
Fracture Toughness ($Mpa \cdot m^{1/2}$)	0.8	6.1

2.2 Drug release

To demonstrate the drug delivery capability of the newly developed device, six tubes with three equidistant holes on their surface were prepared. The length and internal diameter of the tubes and the diameter of the holes were 20 mm, 125 μm and 20 μm respectively. Ethinyl estradiol (EE) was used as model drug in this study. Due to the micro-scale nature of the devices, drug loading is challenging with conventional methods. The drug loading and drug release protocols were followed according to our first study (Rastogi et al. 2010). Briefly, a highly concentrated solution of EE in ethanol (160 mg/ml) was prepared by heating to 80°C. The solution was then loaded into tubes by capillary force. After the evaporation of alcohol, EE was left inside the tube in solid form. The amount of drug loaded into each tube was weighted by thermo-gravimetric analyzer (TGA). The ends of the tubes were plugged with stainless steel

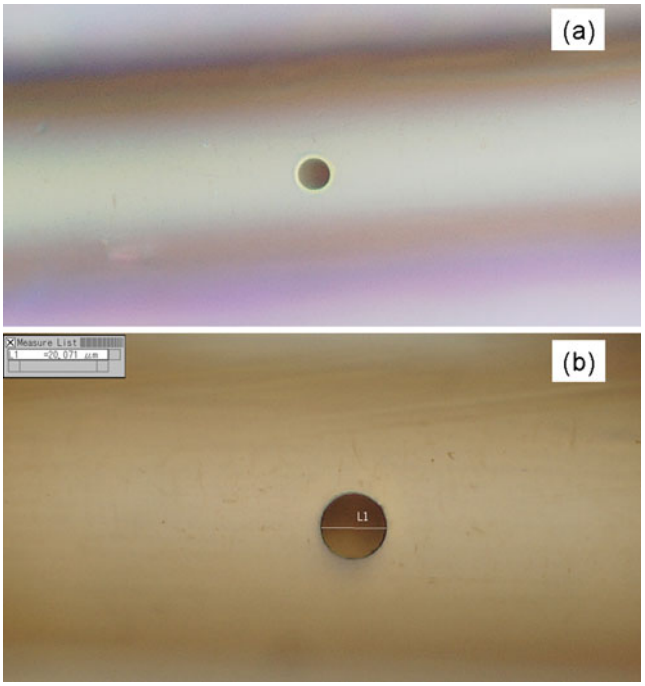

Fig. 6 A 20 μm hole etched on a polyimide tube with SiN_x as etching mask before (**a**) and after (**b**) SiN_x is removed

wires of 120 μm in diameter and sealed with biocompatible glue.

The release study was performed in 0.01 M phosphate buffered saline (PBS) (pH 7.1) in microvials at 37.0±1.0°C. The microvials were placed on a rocker rotating at 46–48 revolutions/min. Enzyme-linked immunosorbent assay (ELISA) based on the competitive reaction where EE competes with the antigen-enzyme conjugate for limited number of binding sites of antibodies was employed to quantitatively measure the EE in samples (AbraxisKits http://www.abraxiskits.com/moreinfo/PN590051USER.pdf). The method is concentration dependent, wherein a sample with higher concentration of EE than the antigen-enzyme conjugate binds more to the antibody producing a lower absorbance. A spectrophotometer operating at 450 nm was used to measure the absorbance.

2.3 Statistical analysis

The SPSS statistical software was used to perform Levene's test to access the homogeneity of variance in various groups. Differences in drug loading were estimated using one way Anova with post hoc analysis using Tukey-HSD test or Games Howell test. Linear regression analysis was performed on the cumulative release data and F-statistics was used to estimate the association between the amount of drug release and time points. A difference of $p<0.05$ was considered significant.

3 Results and discussion

The hole size of the tube manufactured by photolithography techniques was measured as 20±1.1 μm (n=18). An average amount of 51.7±4.8 μg of ethinyl estradiol was loaded inside the tubes (n=6). The data of cumulative amount of EE release over 30 days is shown in Fig. 7. The linearity of the data demonstrates a zero order release. The slope of the line, i.e., the release rate is 32.7±7.3 ng/day (n=6). By extrapolating the data, a sustainable drug release rate of up to 4 years can be reached.

From Fick's law of diffusion, an analytical expression for drug release rate can be derived as

$$dM/dt = (D \bullet C_s/L) \bullet A, \quad (1)$$

where D is the diffusion coefficient, C_s is the solubility of drug, L is the tube wall thickness, and A is the total area of three holes etched on the surface. This zero order release is maintained as long as the drug inside the tube is not totally dissolved. The result in Fig. 7 indicate a linear dependence of release rate on the surface area A. In this device, the size and the number of the hole can be defined by the photomask design to tune the drug release rate.

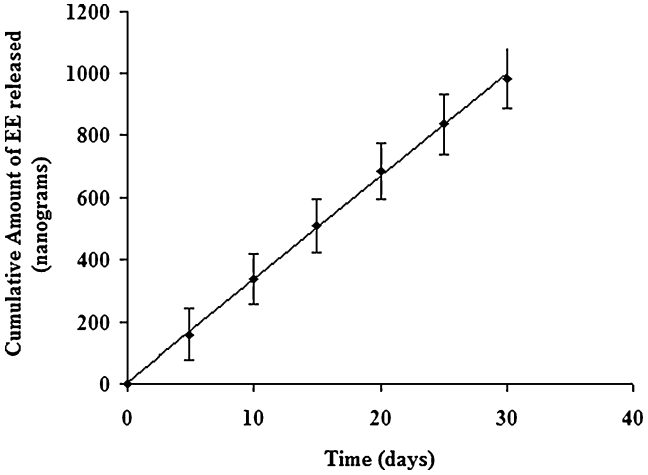

Fig. 7 Cumulative Amount of EE released from microperforated micro tubes fabricated using microfabrication technology over a period of 30 days. The solid line represents the regression line. The average amount of drug released per day is calculated from the slope of the line. The data is represented as mean with standard deviation, n=6

The long term zero order drug release up to years from the perforated devices has the potential to be used to treat various chronic diseases. With the long term drug release, frequent treatment and hospitalization of the patient can be eliminated to improve the patient compliance and quality of life. Multiple tubes can also be used to deliver multiple therapeutic agents with different release rates.

The microfabrication technique developed in this work provides several advantages over laser ablation technique, which can also be used to drill microholes on polyimide tubes. First, photolithography and etching are parallel processes while laser ablation is serial. Using micro-fabrication, the time and cost to fabricate thousands of holes are similar to fabricate one single hole. So the manufacturing cost can be significantly reduced in mass production. Second, the laser ablation technology is normally limited to drill holes larger than about 10 μm while the state of the art lithography in microelectronics industry can produce feature size below 100 nm (ITRS 2009). Finally, the microfabrication technique is not limited to fabrication of microholes. It can be extended to other useful applications, including precise tubing cutting, surface treatment with plasma and surface coating with thin films to functionalize the surface. In particular, it has the potential to integrate sensors and electronics to make smart tubes to deliver drugs in highly controlled complex dosing patterns.

4 Conclusion

A method to fabricate polymer drug deliver devices based on micro-fabrication technology has been developed. The

device fabricated in this study was a polyimide tube with micro-fabricated holes on one surface. A Si platform with trenches and alignment marks was developed to hold the miniature tubes for further processing. Photolithography was applied to define patterns of holes and RIE with ICP source was used to etch holes on polyimide surface. Biocompatible materials Ti, SiO_2 and SiN_x were studied as mask materials. Ti film deposited by e-beam evaporation cannot cover the tube edges well and more conformal film was achieved using SiO_2 and SiN_x deposited by HDPCVD at room temperature. SiN_x was found to be more effective in suppressing crack formation compared to SiO_2 due to its superior thermal and mechanical properties.

Drug loading was achieved using capillary methods. Release of EE was quantitatively measured by ELISA for 30 days with a zero order release rate at 32.7±7.3 ng/day. This long term zero order local drug delivery together with its minimal invasion nature suggests that the device can be used for a variety of applications for chronic disease treatment.

Further investigations are underway, including fabrication of devices on other polymer materials, especially biodegradable polymer, release study for different drugs and with different device geometries, possible electronics integration into the devices.

References

R. Baker, *Controlled release of biologically active agents* (Wiley, New York, 1987)

M. Bessonov, M. Koton, V. Kudryavtsev, L. Laius, *Polyimides: thermally stable polymers* (Consultants Bureau, New York, 1987)

T. Desai, D. Hansford, L. Kulinsky, A. Nashat, G. Rasi, J. Tu, Y. Wang, M. Zhang, M. Ferrari, Biomed Microdevices **2**(1), 11–40 (1999)

J. Dolbow, M. Gosz, Mech Mater **23**(4), 311–322 (1996)

C. Feger, M. Khojasteh, S. Molis, *Polyimides: trends in materials and applications* (Society of Plastics Engineers, New York, 1996)

V. Hatty, H. Kahn, A. Heuer, J MEMS **17**(4), 943–947 (2008)

A. Hillery, A. Lloyd, J. Swarbrick, *Drug delivery and targeting for pharmacists and pharmaceutical scientists* (Taylor & Francis, London, New York, 2001)

J. Hutchinson, Z. Suo, Adv Appl Mech **29**, 63–191 (1992)

ITRS, International Technology Roadmap for Semiconductors (2009) Ed Lithography http://www.itrs.net/Links/2009ITRS/2009Chapters_2009Tables/2009_Litho.pdf

B. Li, M. Kang, K. Lu, R. Huang, P. Ho, R. Allen, M. Cresswells, Nano Lett **8**(1), 92–98 (2008)

J. Maloney, S. Uhland, B. Polito, N. Sheppard, C. Pelta, J. Santini, J Control Release **109**(1-3F), 244–255 (2005)

F. Martin, R. Walczak, A. Boiarski, M. Cohen, T. West, C. Cosentino, M. Ferrari, J Control Release **102**(1), 123–133 (2005)

M. Niwa, H. Kawakami, M. Kanno, S. Nagaoka, T. Kanamori, T. Shinbo, S. Kubota, J Biomater Sci Polym Ed **12**(5), 533–542 (2001)

M. Ohring, *The materials science of thin films: deposition and structure* (Academic Press, San Diego, 2002)

A. Rastogi, Z. Luo, Z .Wu, P. Ho, P. Bowman, S. Stavchansky, Biomed Microdevices **12**(5), 915–921, (2010)

J. Robinson, V. Lee, *Controlled drug delivery: fundamentals and applications* (Marcel Dekker, New York, 1987)

P. Rousche, D. Pellinen, D. Pivin, J. Williams, R. Vetter, D. Kirke, IEEE Trans Biomed Eng **48**(3), 361–371 (2001)

J. Santini, M. Cima, R. Langer, Nature **397**(6717), 335–338 (1999)

J. Santini Jr., A. Richards, R. Scheidt, M. Cima, R. Langer, Angew Chem Int Ed **39**(14), 2396–2407 (2000)

T. Tang, S. Smith, B. Flynn, J. Stevenson, A. Gundlach, H. Reekie, A. Murray, D. Renshaw, B. Dhillon, A. Ohtori, IET Nanobiotechnol **2**(3), 72 (2008)

T. Tsui, A. McKerrow, J. Vlassak, J Mater Res **20**(9), 2266 (2005)

G. Voskerician, M. Shive, R. Shawgo, H. Recum, J. Anderson, M. Cima, R. Langer, Biomaterials **24**(11), 1959–1967 (2003)